Supporting Information

Pure organic quinacridone dyes as dual sensitizers in tandem photoelectrochemical cells for unassisted total water splitting

Luze Shen‡[a], Shicong Zhang‡[a], Haoran Ding[a], Fushuang Niu[b], Yanmeng Chu[c], Wenjun Wu*[a], Yue Hu[c], Ke Hu*[b], Jianli Hua*[a]

[a] *Key Laboratory for Advanced Materials & Institute of Fine Chemicals, College of Chemistry and Molecular Engineering, East China University of Science and Technology, 130 Meilong Rd., Shanghai 200237, China*

[b] *Department of Chemistry, Fudan University, 220 Handan Road, Shanghai 200433, P. R. China.*

[c] *Michael Grätzel Center for Mesoscopic Solar Cells, Wuhan National Laboratory for Optoelectronics, Huazhong University of Science and Technology, 1056 Luoyu Road, Wuhan 430074, Hubei, P. R. China.*

**E-mail: jlhua@ecust.edu.cn; wjwu@ecust.edu.cn*

**E-mail: khu@fudan.edu.cn*

Table of Contents

Reagents and Measurements

Quinacridone, 1-iodobutane, 1-bromo-n-octane, 1-bromohexadecane, Tetrabutylammonium bromide, N-bromosuccinimide (NBS), Bis (pinacolato) diboron, [1,1'-Bis (diphenylphosphino) ferrocene]dichloropalladium(II) (Pd(dppf)Cl_2), Potassium acetate, Potassium phosphate, 2,6-Pyridinedicarboxylicacid, Sodium iodide, N, N-dimethylformamide, Isopropanol and 1,4-dioxane were all purchased from Energy Chemical. All solvents were of reagent grade and used as received without further purification. Our group has successfully synthesized **QAP-C4** and **QAP-C8** for hydrogen generation[1]. The synthesis of the **Co2** and **RuOEC** were prepared as reported in the literature[2].

Preparation of QAP-C16 molecule

Synthesis of compound **QAP-C16**.

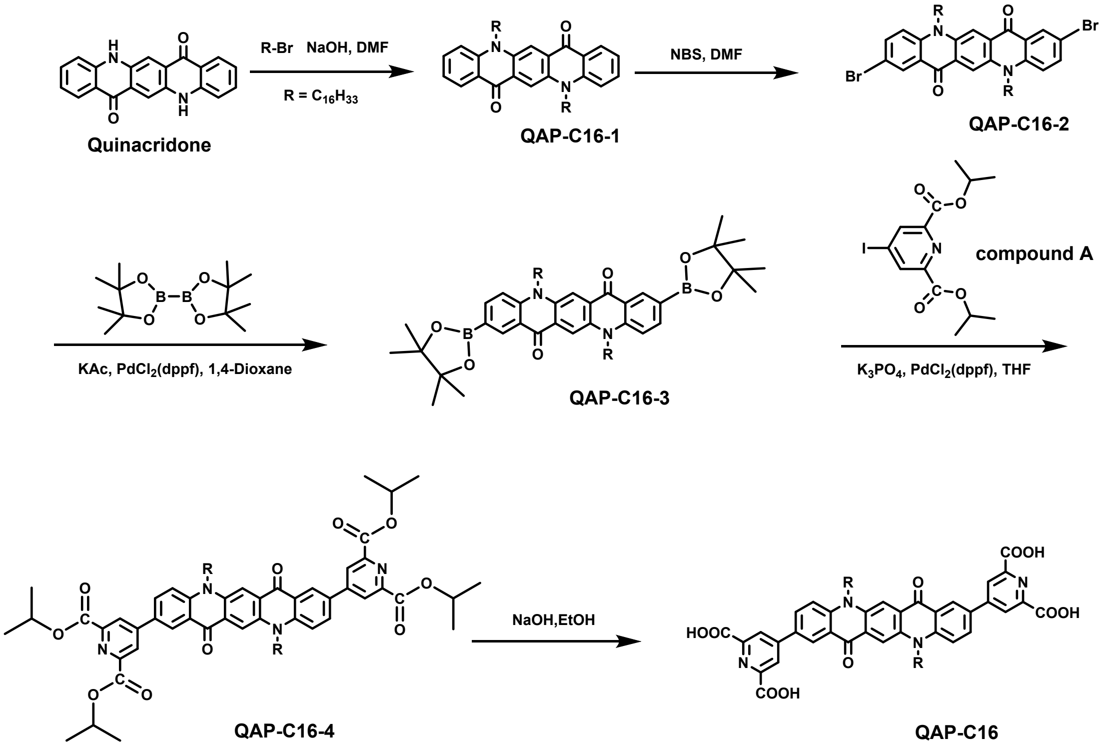

Scheme 1. Synthesis of **QAP-C16**.

Synthesis of QAP-C16-1. Firstly, quinacridone (4.68 g, 15 mmol), NaOH (12 g, 207 mmol), tetrabutylammonium bromide (1 g, 3 mmol) were weighed and transferred into a 250 ml three-necked flask with DMF (120 mL). The solution was flushed with argon and heated at 50 °C for 1-2 h until

$C_{16}H_{33}Br$ (64 mL, 207 mmol) was added. Then the temperature was raised to 100 °C and maintained for 6 h. After the solution was cooled to room temperature, it was poured into a large amount of water and stirred vigorously. Finally, the solution was suction filtered and dried to give a red solid **QAP-C16-1**. Yield: 8.55 g (75%).

^{1}H NMR (400 MHz, Chloroform-*d*) δ 8.81 (s, 2H), 8.60 (dd, *J* = 8.0, 1.8 Hz, 2H), 7.78 (ddd, *J* = 8.7, 7.0, 1.8 Hz, 2H), 7.55 (d, *J* = 8.8 Hz, 2H), 7.31 (d, *J* = 7.5 Hz, 2H), 4.53 (t, *J* = 8.2 Hz, 4H), 2.01 (d, *J* = 7.3 Hz, 4H), 1.47 (s, 4H), 1.26 (s, 48H), 0.88 (t, *J* = 6.7 Hz, 6H).

^{13}C NMR (101 MHz, $CDCl_3$) δ 178.15, 142.26, 135.73, 134.62, 128.08, 126.31, 121.11, 120.83, 114.59, 113.48, 77.38, 77.06, 76.75, 63.77, 59.90, 51.32, 29.69, 29.67, 29.61, 29.47, 29.37, 29.23, 27.64, 27.49, 26.25, 22.79, 22.70, 14.13.

Synthesis of QAP-C16-2. QAP-C16-1 (2.84 g, 2 mmol) and NBS (4.2 g, 24 mmol) were transferred into a single-necked flask and dissolved in DMF (20 mL). The solution was flushed with argon and then reacted in the dark at 60 °C for 12 h. After the solution was cooled to room temperature, water was added and stirred for 30 minutes. After removed DMF and water by rotary evaporation, it was extracted with dichloromethane. The dichloromethane phase was rotary evaporated. The product **QAP-C16-2** was obtained by column chromatography, PE/DCM (2:1 v/v). Yield: 2.40 g (70%).

^{1}H NMR (400 MHz, Chloroform-*d*) δ 8.60 (s, 2H), 8.55 (d, *J* = 2.4 Hz, 2H), 7.76 (dd, *J* = 9.2, 2.5 Hz, 2H), 7.34 (d, *J* = 9.3 Hz, 2H), 4.51 – 4.36 (m, 4H), 1.99 – 1.88 (m, 4H), 1.48 – 1.42 (m, 4H), 1.26 (s, 48H), 0.88 (t, *J* = 6.8 Hz, 6H).

^{13}C NMR (101 MHz, $CDCl_3$) δ 176.61, 140.74, 137.28, 135.35, 130.16, 125.96, 121.96, 116.72, 114.10, 113.68, 77.34, 77.02, 76.71, 31.94, 29.73, 29.69, 29.63, 29.60, 29.45, 29.38, 27.07, 26.98, 22.71, 14.14.

Synthesis of QAP-C16-3. QAP-C16-2 (780 mg, 0.85 mmol), bis(pinacolato)diboron (890 mg, 3.50 mmol), Pd(dppf)Cl_2 (180 mg, 0.25 mmol) and potassium acetate (185 mg, 1.89 mmol) were weighed into a 100 mL Shrek tube, dissolved with 1,4-dioxane (15 mL). Solution was flushed with argon and heated to 80 °C for 8 h. After the solution was cooled to room temperature, the liquid was removed by rotary evaporation. After the solid was extracted with water and dichloromethane, the dichloromethane phase was rotary evaporated. The product **QAP-C16-3** was obtained by column chromatography, DCM/EA (20:1 v/v). Yield: 600 mg (70%).

^{1}H NMR (400 MHz, Chloroform-*d*) δ 9.06 (d, *J* = 1.5 Hz, 2H), 8.79 (s, 2H), 8.13 (dd, *J* = 8.7, 1.5 Hz, 2H), 7.49 (d, *J* = 8.8 Hz, 2H), 4.52 (d, *J* = 7.3 Hz, 4H), 2.03 – 1.98 (m, 4H), 1.46 (dt, *J* = 11.6, 5.5 Hz, 4H), 1.39 (s, 24H), 1.26 (s, 48H), 0.87 (t, *J* = 6.8 Hz, 6H).

^{13}C NMR (101 MHz, $CDCl_3$) δ 178.06, 165.99, 143.97, 140.03, 136.08, 135.77, 134.22, 129.50, 126.66, 120.49, 113.78, 83.93, 83.52, 83.05, 77.36, 77.04, 76.73, 75.06, 67.77, 46.23, 38.89, 31.94, 30.57, 29.71, 29.68, 29.64, 29.61, 29.47, 29.38, 28.99, 27.12, 26.99, 25.03, 24.94, 24.86, 24.58, 23.98, 22.98, 22.71, 14.15, 14.07, 11.10.

Synthesis of QAP-C16-4. QAP-C16-3 (400 mg, 0.40 mmol) and Pd(dppf)Cl_2 (90 mg, 0.12 mmol) were transferred into a two-necked flask and protected with argon. K_3PO_4 (300 mg, 1.41 mmol) was weighed out and dissolved in water (3 mL). After flushed with N_2, K_3PO_4 solution was poured into the flask through syringe. The system was heated to 50 °C for 30 minutes. **Compound A** (470 mg, 1.25 mmol) was dissolved in THF (15 mL) and poured into the flask with syringe. The system was heated to 80 °C for 4 h, and the solution was observed to turn purple-red. After the solution was cooled to room temperature, the liquid was removed by rotary evaporation. After the solid was extracted with water and dichloromethane, the dichloromethane phase was rotary evaporated. The product **QAP-C16-4** was obtained by column chromatography, DCM/EA (20:1 v/v). Yield: 368 mg (77%).

^{1}H NMR (400 MHz, Chloroform-*d*) δ 8.99 (d, *J* = 2.3 Hz, 2H), 8.83 (s, 2H), 8.57 (s, 4H), 8.18 (dd, *J* = 9.1, 2.3 Hz, 2H), 7.73 (s, 2H), 5.39 (hept, *J* = 6.2 Hz, 4H), 4.70 – 4.52 (m, 4H), 2.06 (d, *J* = 6.8 Hz, 4H), 1.68 (p, *J* = 7.2 Hz, 4H), 1.50 (d, *J* = 6.3 Hz, 24H), 1.25 (s, 48H), 0.87 (t, *J* = 6.8 Hz, 6H).

^{13}C NMR (101 MHz, $CDCl_3$) δ 177.75, 164.25, 163.76, 150.33, 149.79, 149.01, 146.67, 142.90, 135.82, 132.79, 128.70, 126.82, 126.49, 125.24, 124.58, 121.25, 116.14, 114.11, 77.37, 77.06, 76.74, 70.80, 70.77, 70.35, 70.33, 46.76, 31.93, 29.71, 29.69, 29.62, 29.51, 29.37, 27.28, 27.09, 22.70, 21.90, 21.84, 14.14.

Synthesis of QAP-C16. QAP-C16-4 (370 mg, 0.30 mmol) and NaOH (500 mg, 12.5 mmol) were weighed into a single-necked flask and dissolved in ethanol (15 mL) and water (2 mL). The system was flushed with argon and heated to 100 °C for 20 h. After the solution was cooled to room temperature, the liquid was removed by rotary evaporation. Adjust the pH of the solution to 1 with dilute hydrochloric acid, and the purple solid was precipitated. After the solution was centrifuged, discarded the supernatant and washed the precipitate with deionized water for three times. **QAP-C16** can be obtained by drying the precipitate. Yield: 300 mg (90%).

The structure of **QAP-C16** was confirmed by FT-IR (Fig. S1). The peak at 1744 cm^{-1} was attributed to the C=O stretching vibration of the PDA. The FT-IR of **QAP-C16** did not show this peak, indicating that all ester groups were hydrolyzed to carboxyl groups. The peak at 1281cm^{-1} was due to the C-N expansion vibration of quinacridone core. And the peak at 1636cm^{-1} was due to the characteristic stretching vibration of C=N of PDA.

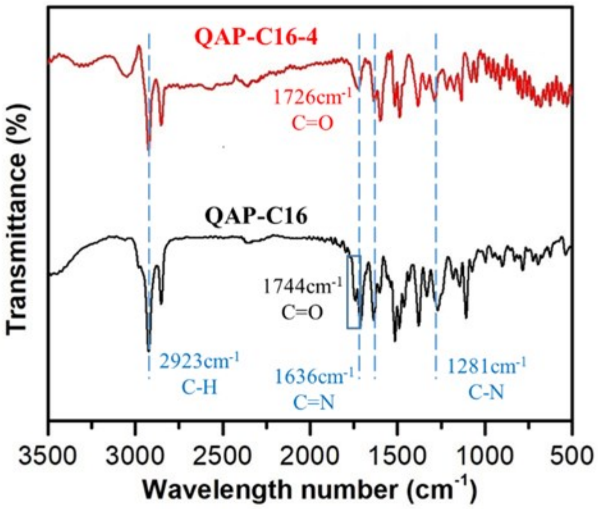

Fig. S1. Fourier transform infrared (FT-IR) spectra of **QAP-C16-4** and **QAP-C16**.

Preparation of the photoelectrodes.

F-doped tin oxide (FTO) -coated conductive glass (Hartford Glass; sheet resistance 15 Ω cm^{-2}) (25 mm × 35 mm) was cleaned by sonication for 30 min in soapy water, deionized water, ethanol and acetone, respectively. After cleaning, FTO glass was stored in ethanol.

Putted tape around the FTO substrate (the exposed area is 10 mm × 20 mm), and applied TiO_2 paste with a doctor blade method. After annealed to 450 °C for 30 min in muffle furnace, film was immersed in a titanium tetrachloride solution (46 mM) at 70 °C for 30 min. After cleaning with deionized water, the film was annealed in a muffle furnace at 450 °C for 30 min. Finally, FTO|TiO_2 film was cut into two 10×35 mm^2 strips (the active area was 10 mm × 10 mm).

NiO precursor solution was prepared by dissolving $NiCl\cdot 6H_2O$ (1.83 g) and F68 (poloxamer, 1.00 g) in a mixture of deionized water (2.17 g) and ethanol (6.00 g). Putted tape around the FTO substrate (the exposed area is 20 mm × 20 mm). The NiO precursor solution was evenly coated on the FTO surface by using spin coater (2000 rpm, 30 seconds). The film was annealed to 450 °C for 20 min by heating stage and then cooled to room temperature. Repeated the above steps 4 times to complete the preparation of FTO | NiO[3].

The field emission scanning electron microscopy (FE-SEM) was used to determine of the structural and morphological characterizations of TiO_2 and NiO films. The FE-SEM images of TiO_2 and NiO nanocrystals are shown in Fig. S2. The shape of TiO_2 nanoparticles is similar to ellipsoidal particles, and the average size is about 25 nm. NiO nanoparticles are spherical in shape with an average size of about 15 nm.

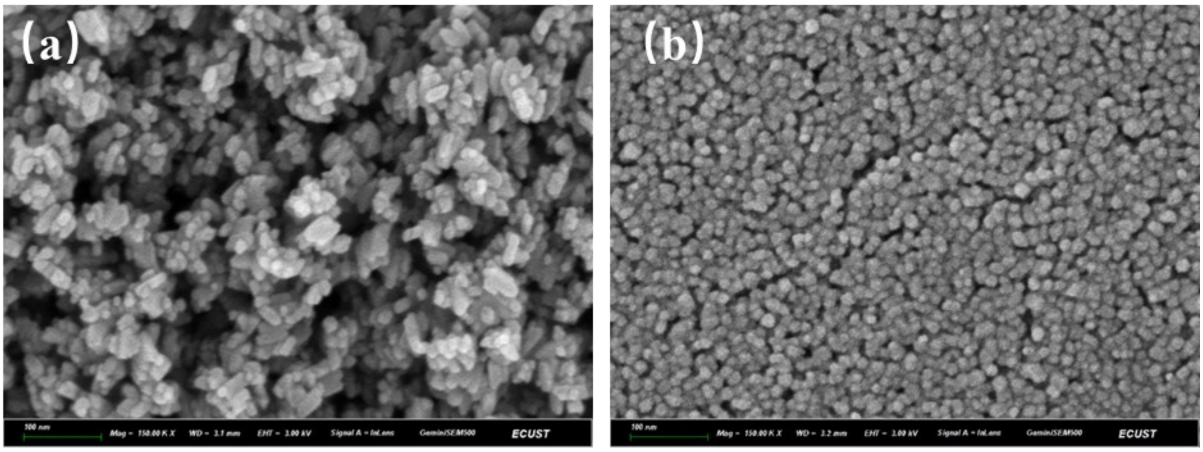

Fig. S2. FE-SEM images of TiO_2 (a) and NiO (b).

TiO_2|QAP was prepared by immersing the bare FTO|TiO_2 into 1 mM QAP DMSO (Dimethyl sulfoxide) solution at 40 °C for 24 h. After rinsed by ethanol, TiO_2|QAP was immersed in 1 mM $ZrOCl_2$ MeOH solution for 10 h to prepare TiO_2 | QAP | Zr^{4+}. Followed by rinsed with ethanol, the film was immersed in 1 mM RuOEC MeOH solution for 10 h, and dried with air to obtain the TiO_2 | QAP |Zr^{4+} | RuOEC electrode. NiO | QAP electrode was prepared by immersing the bare FTO | NiO in 1 mM QAP DMSO solution at 40 °C for 24 hours. After rinsed by ethanol, NiO | QAP electrode was immersed in 1 mM Co2 MeOH solution for 4 h to prepare NiO | QAP+Co2 electrode.

Collector−Generator electrode Fabrication.

The collector−generator electrode included two FTO-based electrodes as working electrodes[3]. One was prepared FTO | TiO_2 | QAP| Zr^{4+} | RuOEC electrode, and the other was bare FTO glass. Cut FTO glass (25 mm × 35 mm) into two strips (10 mm × 20 mm). Then cut the strips along the line between the top midpoint and the side midpoint. Two 1 mm thick and 1 mm wide microscope slides cut in advance were placed on both sides of the bare FTO. Then attached the prepared strips, made the conductive surfaces opposite. The joints were bonded with epoxy-based cement.

Photoelectrochemical measurements.

Photoelectrochemical measurements were performed in a custom made two-compartment photoelectrochemical cell. Measurements were operated with LED light source (λ > 400 nm, 100 mW/cm^2, Color temperature 6500K). A CHI 650E potentiostat was used to apply bias voltage to the working electrode and record the current–time (i-t), cyclic voltammetry (CV), spectroelectrochemical measurements, LSV, impedance and Incident photon to current conversion efficiency (IPCE) signals. Measurements of three-electrode system used prepared FTO film as working electrode, platinum wires as photocathode. I-t, LSV, impedance and IPCE measurements used saturated Ag/AgCl (saturated KCl solution) as reference electrode and phosphate solution (pH=7, 0.1 M) as buffer solution. CV measurements used calomel electrode as reference electrode and tetrabutylammonium hexafluorophosphate tetrahydrofuran (THF) solution as buffer solution.

Faradaic efficiency (η_{oxygen}) for O_2 production can be expressed by the equation[4] (1):

$$\eta_{oxygen}\,(\%) = \frac{Q_{Collector}}{Q_{Generator} \times 0.7} \times 100\% \qquad (1)$$

Where $\frac{Q_{Collector}}{Q_{Generator}}$ is the ratio of charge at the collector electrode and generator electrode, 0.7 is the efficiency of the collector electrode to collect oxygen. For TiO_2|QAP-C8|Zr^{4+}|RuOEC electrode, photocurrent density of collector electrode reached plateaus at 2.7 μA·cm^{-2} with 0.048 C (**Fig. 3d**) charge passing through. TiO_2|QAP-C8|Zr^{4+}|RuOEC electrode produced 0.50 μmol O_2 with 0.207 C (**Fig. 3b**) charge passing through. Faraday efficiency was calculated to be 33%.

For TiO_2|QAP-C16|Zr^{4+}|RuOEC electrode, photocurrent density of collector electrode reached plateaus at 2.8 μA·cm^{-2} with 0.044 C (**Fig. 3d**) charge passing through. TiO_2|QAP-C16|Zr^{4+}|RuOEC electrode produced 0.46 μmol O_2 with 0.233 C (**Fig. 3b**) charge passing through. Faraday efficiency was calculated to be 27%.

Faradaic efficiency ($\eta_{hydrogen}$) for O_2 production can be expressed by the equation (2):

$$\eta_{hydrogen}(\%) = \frac{2 \times e \times N_A \times n_{H_2}}{Q} \times 100\% \qquad (2)$$

Where e is the elementary charge, N_A is the Avogadro constant, $\eta_{hydrogen}$ is the amount of hydrogen, and Q is the amount of the passing charge in 15 minutes. After 15 minutes of illumination, 1 mL of gas was extracted from the photocathode chamber and analyzed by gas chromatography. In 1 mL of gas, 8.58 nmol of hydrogen was detected. The total volume of gas in the photocathode chamber is 50 mL. So, the total hydrogen production is 429 nmol. The average current in 15 minutes is 104 $\mu A \cdot cm^{-2}$, and the charge passing through is 0.0936 C. The calculated Faraday efficiency is 89%.

IPCE can be expressed by the equation[4] (3):

$$IPCE(\%) = \frac{1240 \times (J_{light} - J_{dark})}{\lambda \times P_{light}} \times 100\% \qquad (3)$$

Where $J_{light} - J_{dark}$ (mA/cm^2) is the measured photocurrent density at a specific wavelength, λ (nm) is the wavelength of incident light, and P_{light} (mW/cm^2) is the measured irradiance at a specific wavelength.

STH can be expressed by the equation (4):

$$STH = \frac{J_{tandem}[mAcm^{-2}] \times (V_{water\ splitting} - V_{bias}) \times \eta_F}{P_{light}[mWcm^{-2}]} \times 100\% \qquad (4)$$

Where J_{tandem} is the average current density of tandem DSPEC cells within 15 mins (104 $\mu A \cdot cm^{-2}$). $V_{water\ splitting}$ is the potential for water splitting (1.23 V). V_{bias} is the bias voltage added to the two electrodes (0 V). η_F is the Faraday efficiency (89%). P_{light} is the intensity of LED light irradiated from two electrodes (100 $mW \cdot cm^{-2}$). According to Eq (8), an STH of tandem DSPEC cells was calculated to be 0.11%.

An A1232c potentiostat was used to record the O_2 generation measurement signals, in which used four-electrode system including prepared FTO as first working electrode, bare FTO as second working electrode, platinum wires as photocathode and saturated Ag/AgCl (saturated KCl solution) as reference electrode. Before the photoelectrochemical measurements, PEC cells were deaerated by argon for 20 min.

P-n tandem measurement was performed in a custom made two-compartment photoelectrochemical cell. We prepared NiO | QAP electrode as the photocathode for p-n series measurement, prepared TiO_2|QAP |Zr^{4+}|RuOEC electrode as the photoanode, and saturated Ag/AgCl (3M KCl) as reference electrode. The compartment of photocathode was deaerated by argon for 20 min. A CHI 650E potentiostat was used to record the signals with no bias voltage. PEC cell was operated with LED light from both compartments.

Electrochemistry section

Ground state oxidation potential ($E_{S+/S}$) and ground state reduction potential ($E_{S-/S}$) can be expressed by the equation (5) and (6):

$$E_{S+/S} = E_{+} + E_{Fc+} + E_{Fc} \tag{5}$$

$$E_{S-/S} = E_{-} + E_{Fc-} + E_{Fc} \tag{6}$$

Where E_{Fc+} is the oxidation onset potential of ferrocene, E_{Fc-} is the reduction onset potential of ferrocene, E_{Fc} is the half-wave potential of ferrocene. Band gap of dyes can be expressed by the equation (7):

$$E_g = \frac{1240}{\lambda} \tag{7}$$

Where λ is intersection of UV-vis spectrum and fluorescence emission spectrum (shown in Figure S4). Excited state oxidation potential ($E_{S*+/S*}$) and excited state reduction potential ($E_{S*-/S*}$) can be expressed by the equation (8) and (9):

$$E_{S*+/S*} = E_{S-/S} + E_g \tag{8}$$

$$E_{S*-/S*} = E_{S+/S} - E_g \tag{9}$$

Cyclic voltammetry curves of three QAP dyes

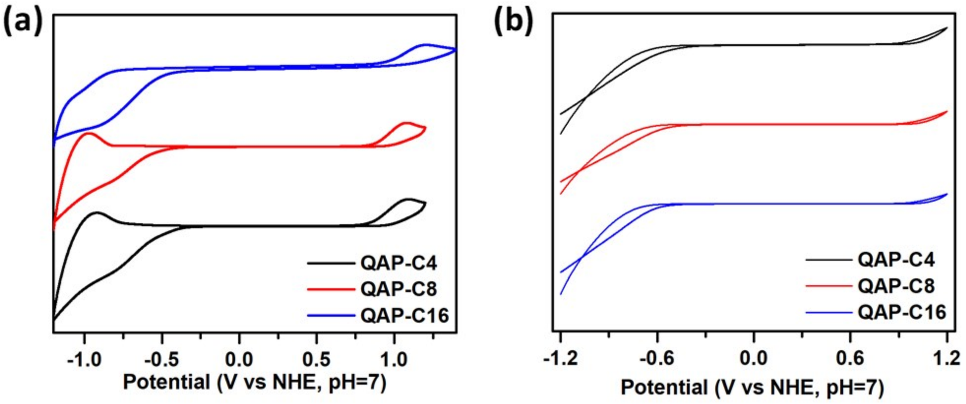

Fig. S3. (a) Cyclic voltammetry curve (CV) of three QAP dyes. (b) CV curve of three QAP dyes, co-adsorption with CDCA. The measurements were conducted in a three-electrode cell with FTO|TiO$_2$|QAP as working electrode, saturated Ag/AgCl as reference electrode and platinum wire as counter electrode. 0.1 M pH = 7 PBS was used as the electrolyte and the CVs were taken at a scan rate of 50 mV/s.

UV-vis spectrums and fluorescence emission spectrums of three QAP dyes

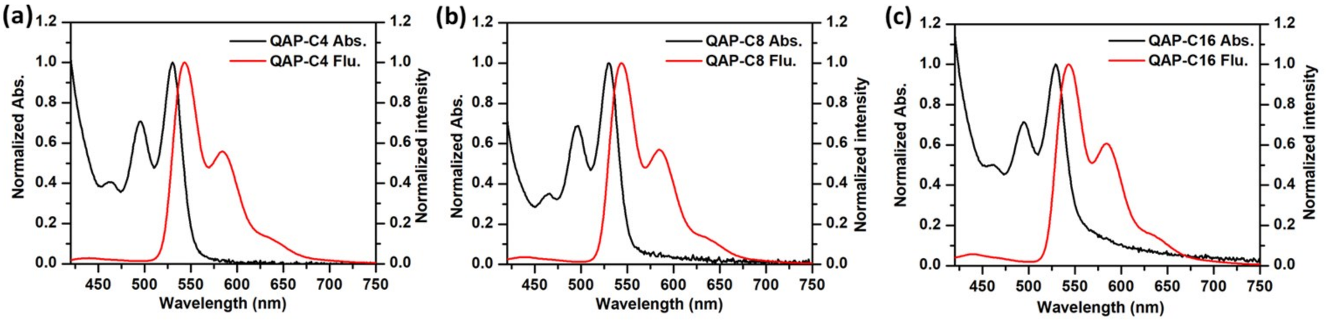

Fig. S4. UV-vis spectrum (black) and fluorescence emission spectrum (red) of **QAP-C4** (a) **QAP-C8** (b) and **QAP-C16** (c) in DMSO.

Spectroelectrochemical of QAP-C8.

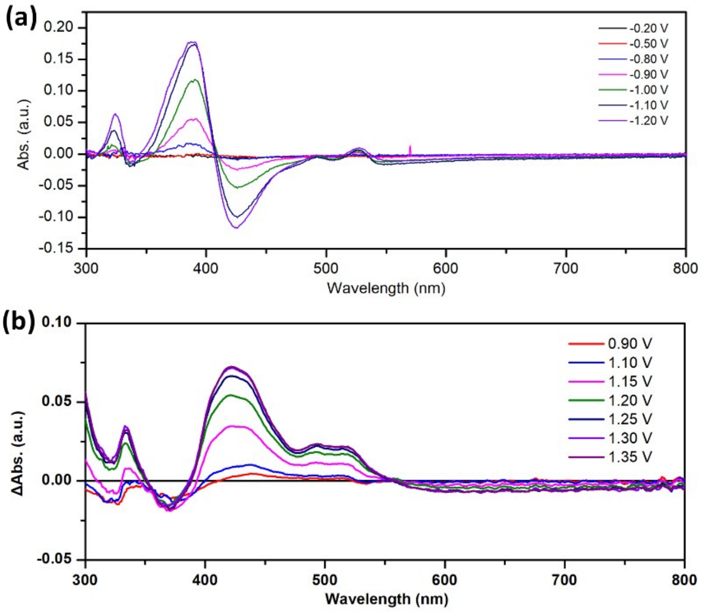

Fig. S5. (a) Spectroelectrochemical reduction of **QAP-C8**. (b) Spectroelectrochemical oxidation of **QAP-C8**.

Photoelectrochemical performance of photoanode based on QAP-C8 and QAP-C16

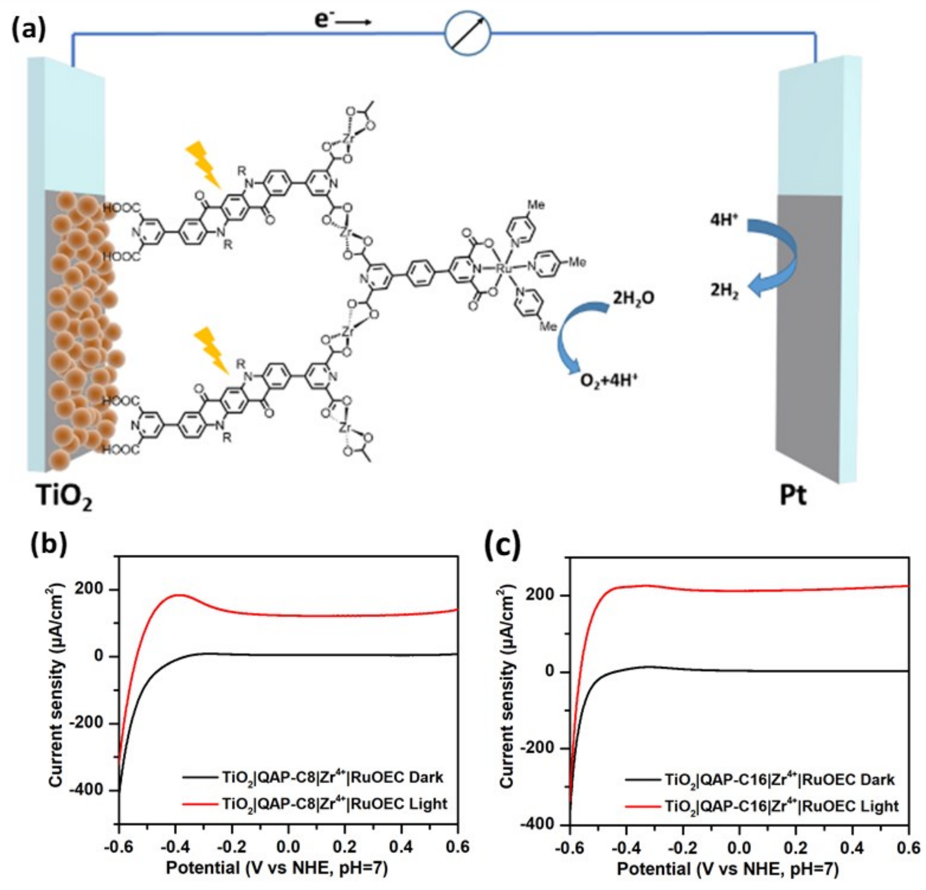

Fig. S6. (a) Schematic diagram of n-DSPEC cell. (b) (c) LSV curves of TiO_2|QAP-C8|Zr^{4+}|RuOEC electrode (b) and TiO_2|QAP-C16|Zr^{4+}|RuOEC electrode (c). Three-electrode PEC cell with Pt as the counter electrode and saturated Ag/AgCl as the reference electrode (light intensity 100 mW·cm^{-2}; scan rate = 50 mV s^{-1}; 0.1 M pH=7.0 phosphate buffer solution).

IPEC spectrums of QAP-C8 and QAP-C16

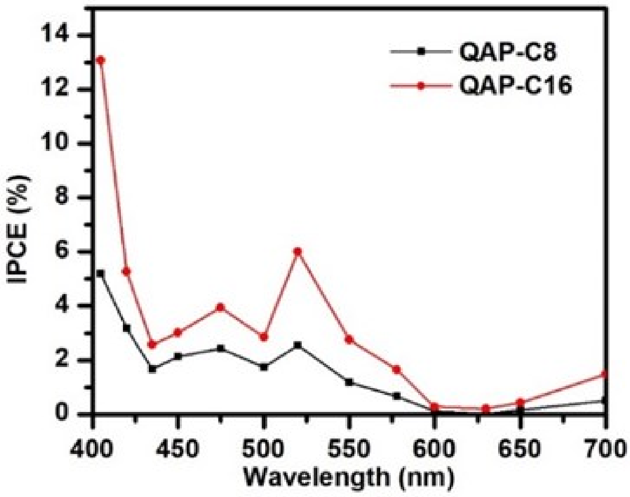

Fig. S7. IPCE curves of **QAP-C8** and **QAP-C16**. Three-electrode PEC cell with Pt as the counter electrode and saturated Ag/AgCl as the reference electrode (light intensity 100 mW·cm^{-2}; bias of 0.2 V vs NHE pH = 7 for **QAP-C8** and 0.3 V vs NHE pH = 7 for **QAP-C16**; 0.1 M pH=7.0 phosphate buffer solution).

Charge (Q)-time curve of the generator and the collector photoanodes

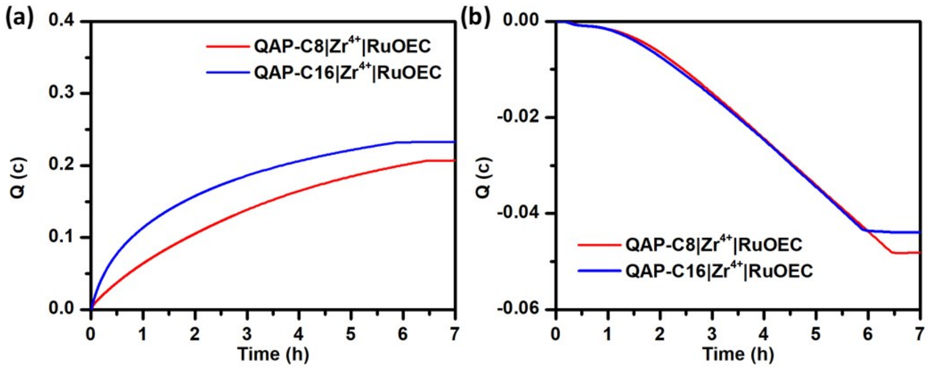

Fig. S8. (a) Charge (Q)-time curve of the oxygen generator photoanode. (b) Charge (Q)-time curve of the oxygen collector electrode. The oxygen generator photoanode is under an applied bias potential of 0.3 V vs NHE (pH = 7), and collector electrode is under an applied bias potential of -0.85 V vs NHE (light intensity 100 mW cm^{-2}; 0.1 M pH=7.0 phosphate buffer solution, with Pt as the counter electrode and saturated Ag/AgCl as the reference electrode).

Photoelectrochemical performance of photocathode based on three QAP dyes

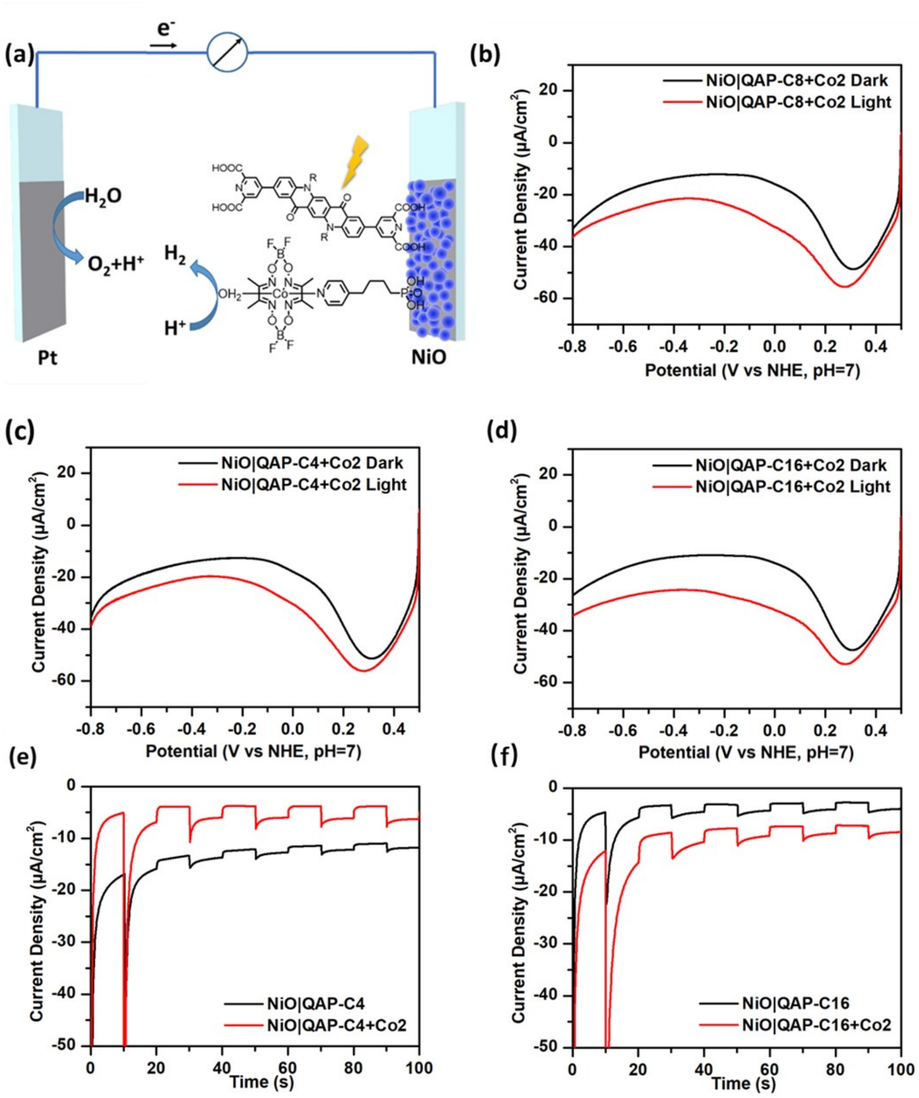

Fig. S9. (a) Schematic diagram of p-DSPEC cell. (b)(c)(d) LSV curves of NiO|QAP-C8+Co2 photocathode (b), NiO|QAP-C4+Co2 photocathode (c) and NiO|QAP-C16+Co2 (d) photocathode in a three-electrode PEC cell (light intensity 100 mW cm^{-2}; scan rate = 50 mV s^{-1}; 0.1 M pH=7.0 phosphate buffer solution), with NiO|QAP-C4+Co2 electrode as photocathode, Pt as a counter electrode, saturated Ag/AgCl electrode as a reference electrode.(e)(f) Transient current responses to on-off cycles of NiO|QAP-C4+Co2 photocathode (e) and NiO|QAP-C16+Co2 photocathode (f) under an applied bias potential of -0.1 V vs NHE (pH = 7) in a three-electrode PEC cells (light intensity 100 mW cm^{-2}; 0.1 M pH=7.0 phosphate buffer solution), with NiO|QAP-C4+Co2 electrode as photocathode, Pt as counter electrode and saturated Ag/AgCl as reference electrode.

Current density (j)-time curve of tandem DSPECs

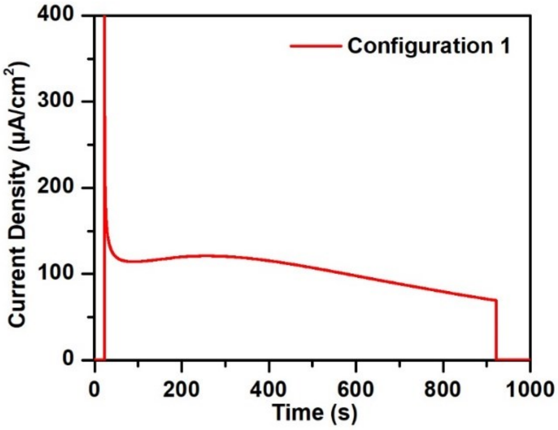

Fig. S10. Current responses of tandem DSPECs under continuous irradiation. Light intensity 100 mW cm^{-2}; scan rate = 50 mV s^{-1}; 0.1 M pH = 7.0 phosphate buffer solution.

The plots of evolved H_2/O_2 yield against irradiation time

The yields of H_2 were 429 nmol, 682 nmol and 743 nmol and the corresponding $\eta_{hydrogen}$ were 89%, 100% and 97% at 15 min, 30 min and 60 min, respectively. The yields of O_2 were 5.6 nmol, 20.5 nmol and 83.9 nmol and the corresponding η_{oxygen} were 2.3%, 6.0% and 21.9%, respectively. At 15 minutes and 30 minutes, the oxygen production and Faraday efficiency are very low for the following reasons: 1) It took time for oxygen to diffuse from the generator electrode to the collecting electrode. 2) A part of oxygen dissolved in water. 3) Oxygen was not the only form of oxidation products.

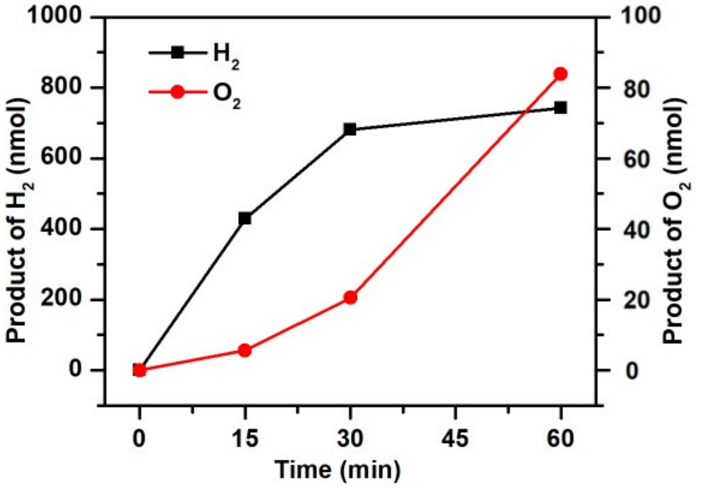

Fig. S11. The plots of evolved H_2/O_2 yield against irradiation time

Theoretical calculation

Methodology: Geometry optimizations were carried out on the molecules in the gas phase, using the software Avogadro[5] to enter the starting geometry. The molecules were distorted to form various conformations, and then the global minimum of the potential energy surface was found through structural optimization. Frequency calculations were performed on the optimized geometry to distinguish whether they are in a minimum state or a transition state on the potential energy surface. Finally, in the transition state structure, the bond length and bond angle were distorted in the vibration direction, and the structure was re-optimized until only positive frequencies were obtained. All calculations were performed using the Gaussian 09 program[6] with the B3LYP function, UB3LYP, and the standard 6-31G (d) basic settings in the Gaussian 09 program[7].

Table S1. Frontier molecular orbitals of the dyes QA-C4、QAP-C4、QAP-C8 and QAP-C16 optimized in vacuum

Dye	HOMO-1	HOMO	LUMO	LUMO+1
QA-C4	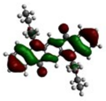 -6.07 eV	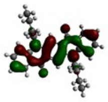 -5.18 eV	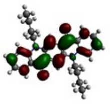 -2.09 eV	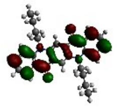 -1.00 eV
QAP-C4	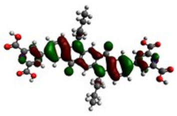 -6.46 eV	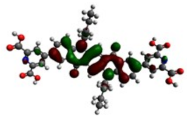 -5.67 eV	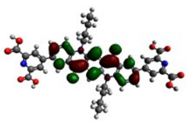 -2.61 eV	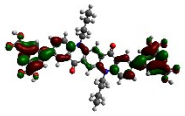 -2.01 eV
QAP-C8	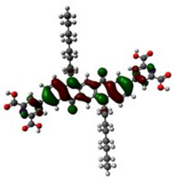 -6.44 eV	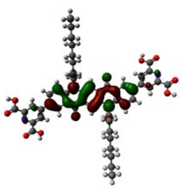 -5.65 eV	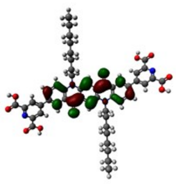 -2.60 eV	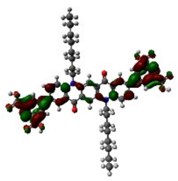 -2.00 eV

QAP-C16	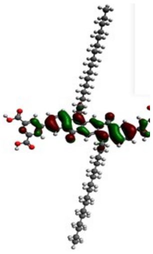 -6.34 eV	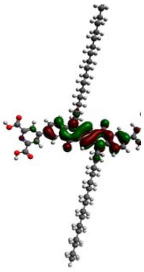 -5.54 eV	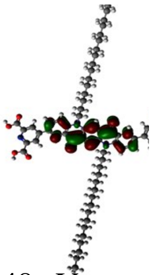 -2.48 eV	1.07 eV 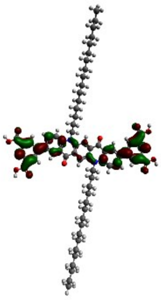

Table S2. TD-DFT calculated energies, oscillator strengths (f), and compositions in terms of molecular orbital contributions of QA-C4, QAP-C4, QAP-C8 and QAP-C16

Dye	Composition[a]	E(nm)	*f*
QA-C4	70% H→L	480	0.1063
QAP-C4	70% H→L	485	0.0798
	70% H→L+1	412	0.8632
QAP-C8	70% H→L	485	0.0831
	70% H→L+1	412	0.8502
QAP-C16	70% H→L	485	0.0854
	70% H→L+1	413	0.8713

[a] H=HOMO, L=LUMO, H-1=HOMO-1

Table s3. Optical and electrochemical properties of the dyes

Dye	λ (nm)	$E_{S+/S}$ (V)	$E_{S/S-}$ (V)	E_g (V)	$E_{S*/S-}$ (V)	$E_{S+/S*}$ (V)
QAP-C4	535.7	1.18	-0.66	2.32	1.66	-1.14
QAP-C8	535.7	1.23	-0.70	2.32	1.62	-1.09
QAP-C16	534.9	1.36	-0.80	2.32	1.52	-0.96

Original spectral copy of new compounds

^{13}C NMR spectrum of **QAP-C16-1** in DMSO-d6.

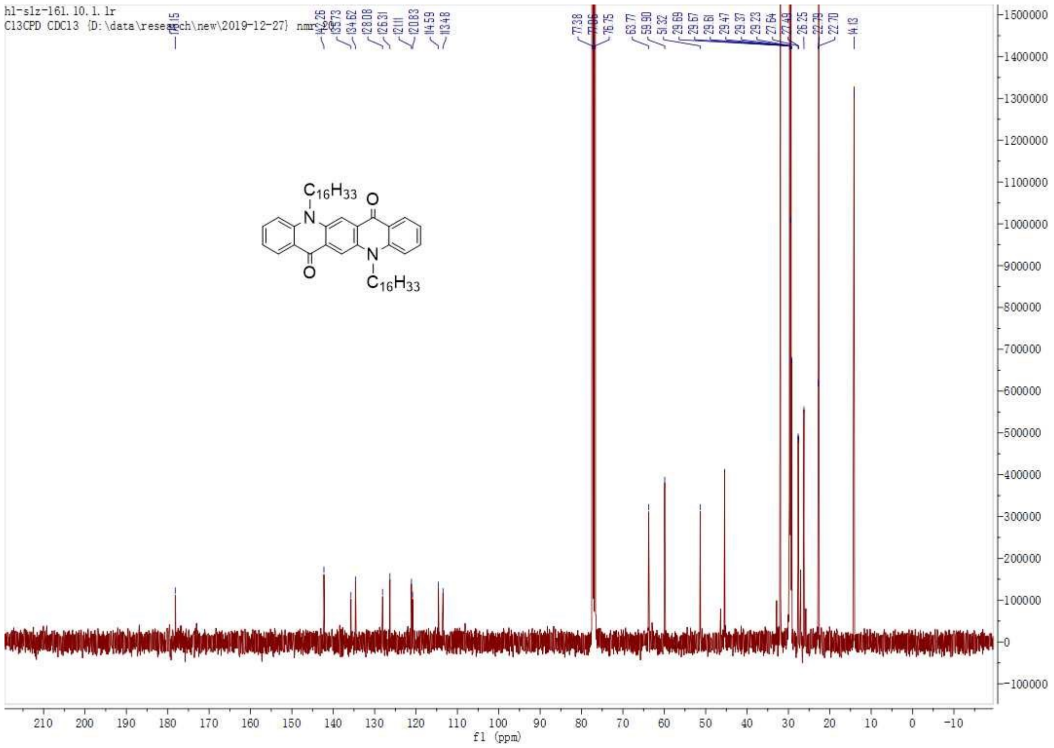

^{1}H NMR spectrum of **QAP-C16-2** in DMSO-d_6.

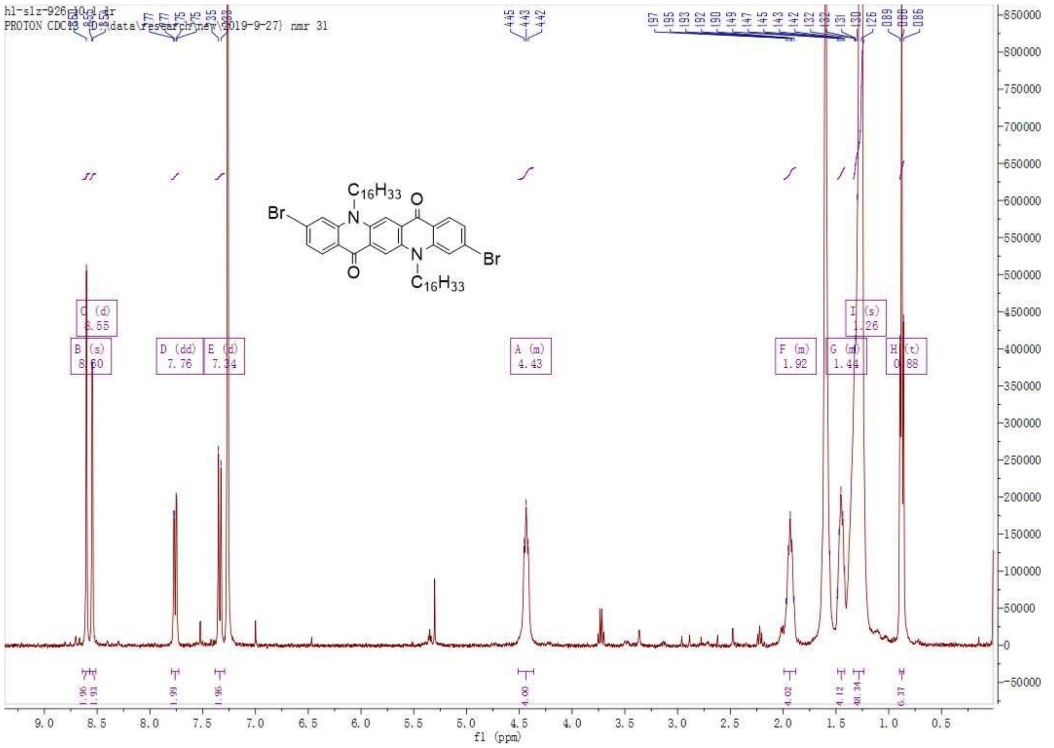

^{13}C NMR spectrum of **QAP-C16-2** in DMSO-d$_6$.

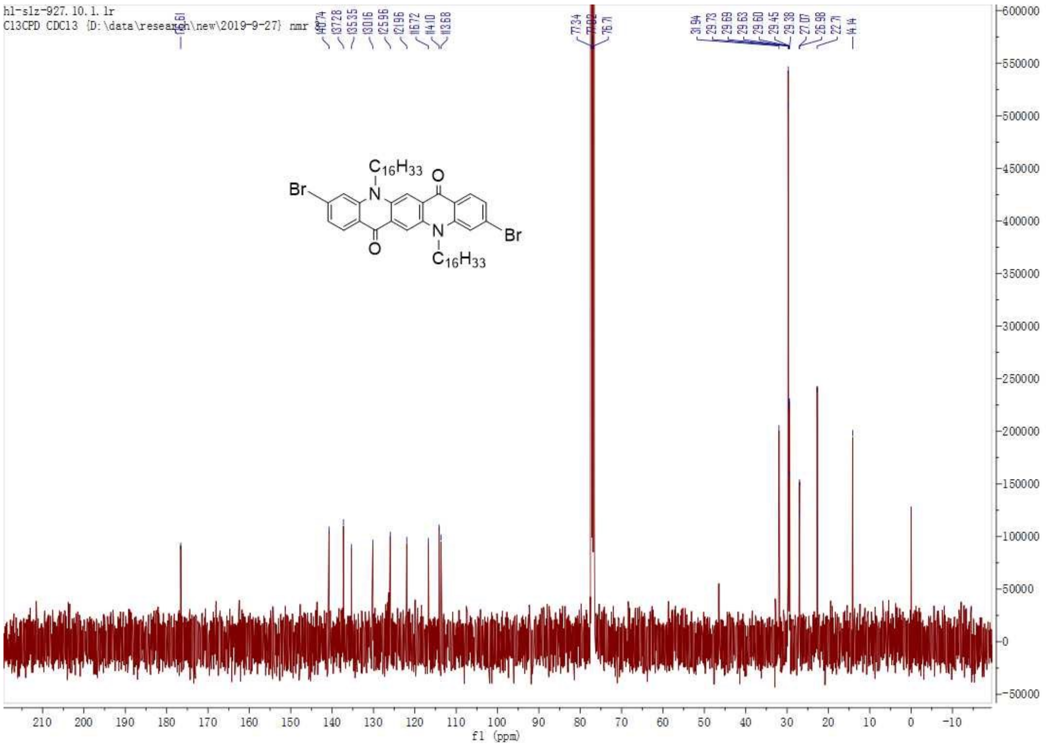

^{1}H NMR spectrum of **QAP-C16-3** in DMSO-d$_6$.

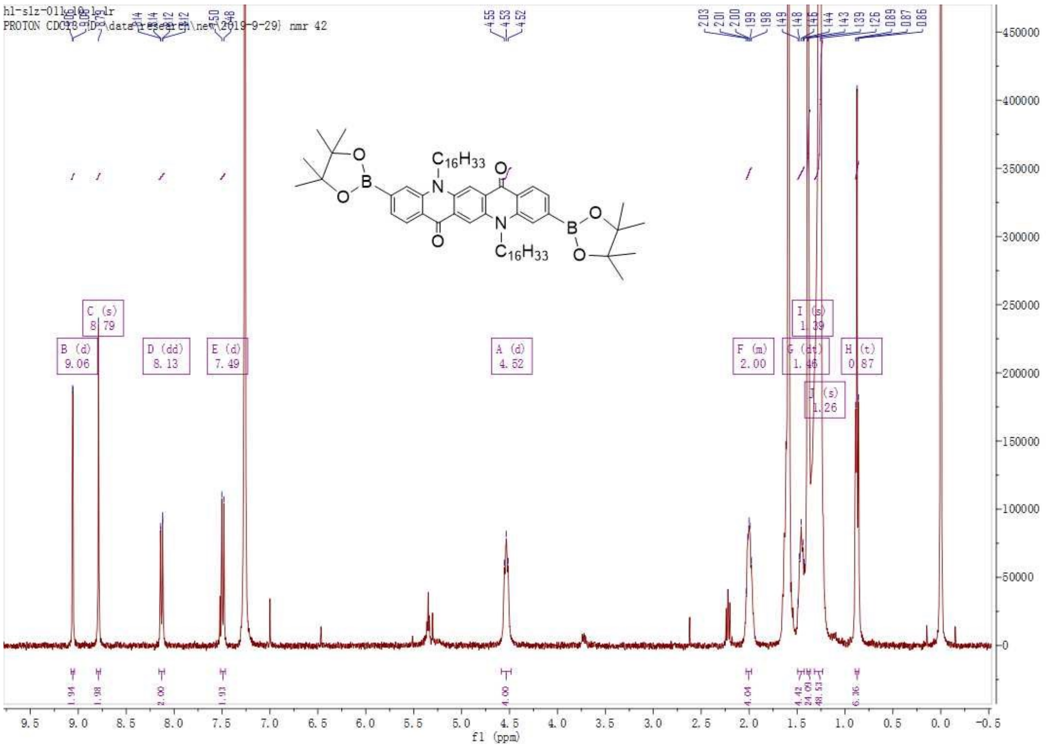

^{13}C NMR spectrum of **QAP-C16-3** in DMSO-d_6.

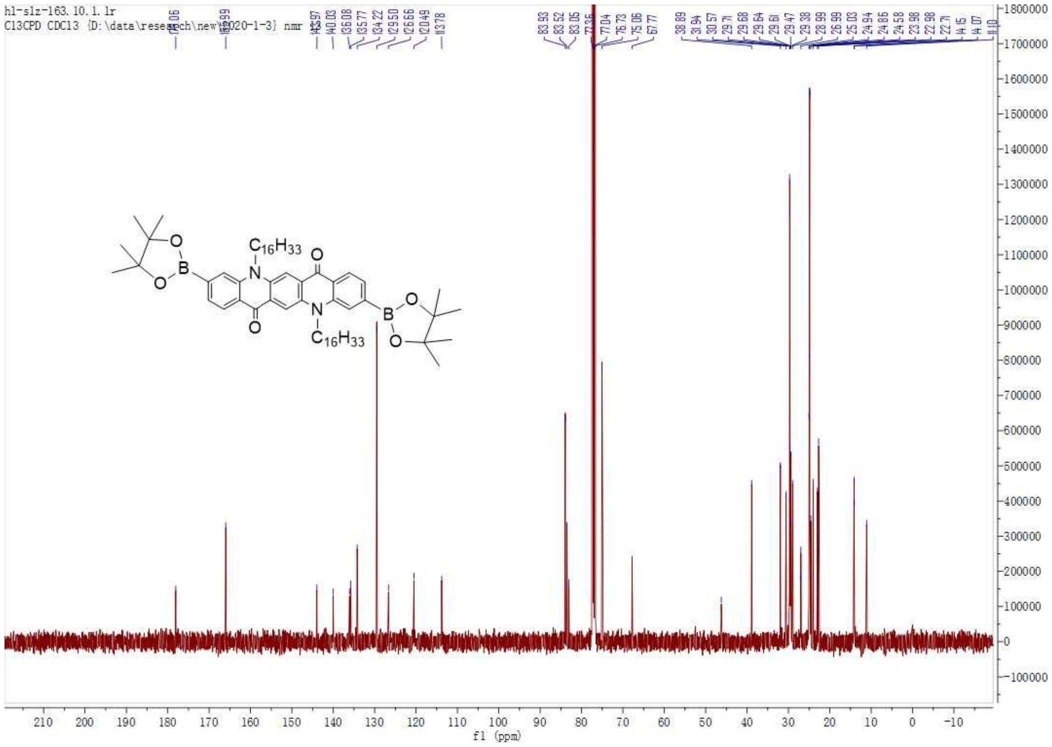

^{1}H NMR spectrum of **QAP-C16-4** in DMSO-d_6.

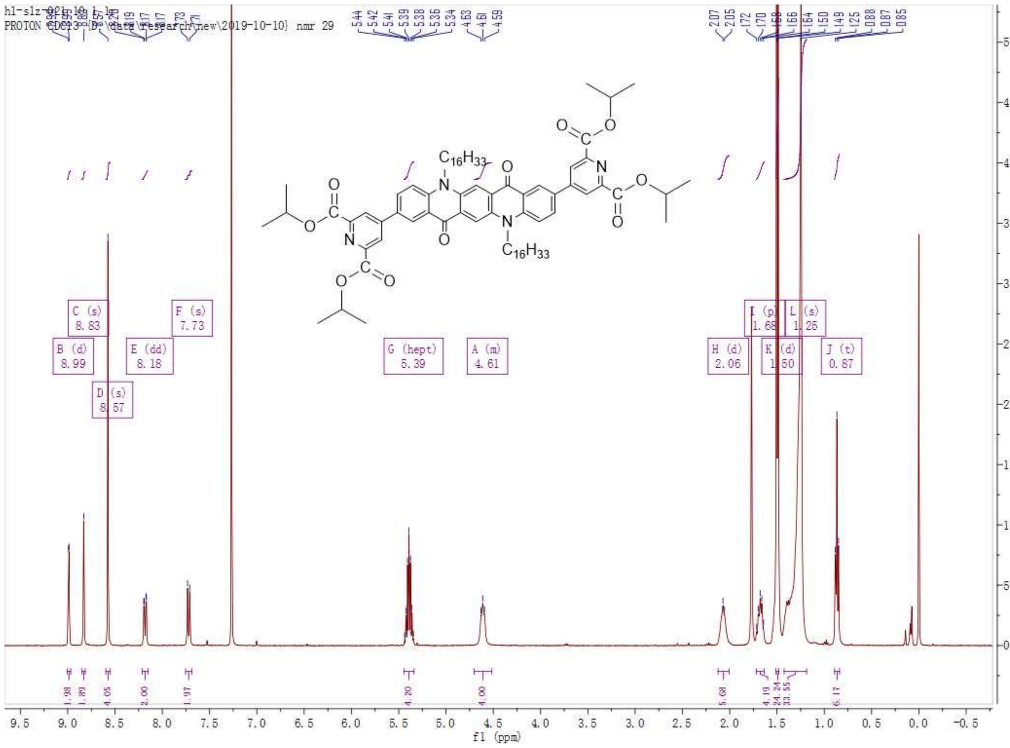

^{13}C NMR spectrum of **QAP-C16-4** in DMSO-d_6.

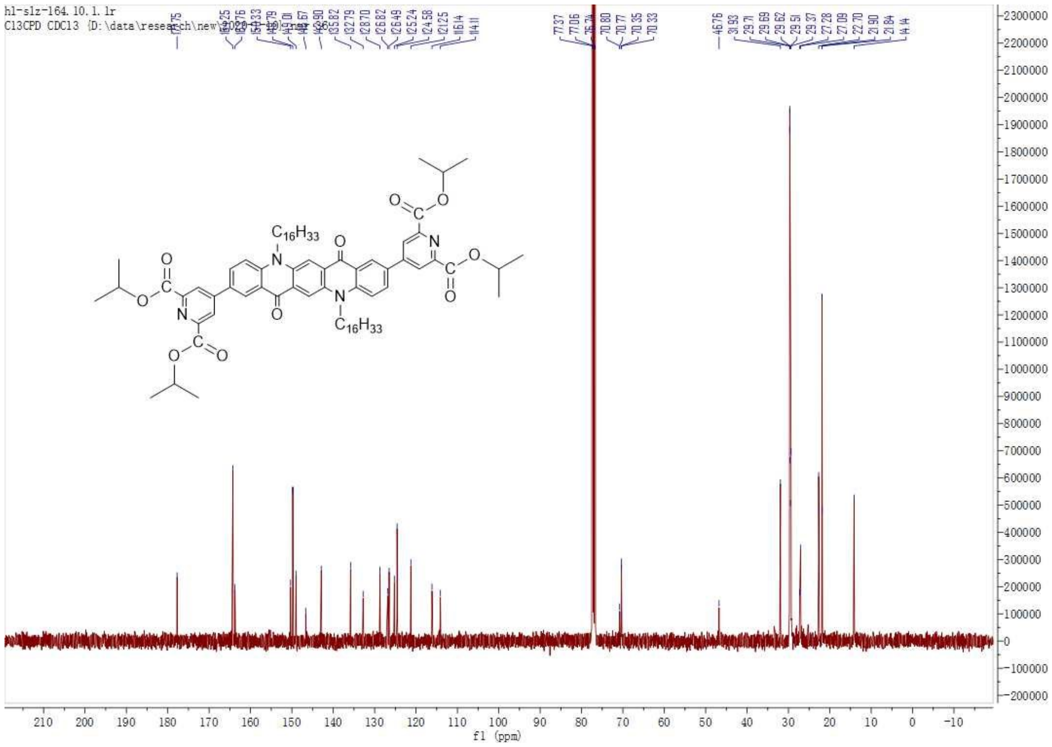

Reference

1. M. Xu, K. Kong, H. Ding, Y. Chu, S. Zhang, F. Yu, H. Ye, Y. Hu and J. Hua, *Journal of Materials Chemistry C*, 2020, **8**, 930-934.
2. F. Li, K. Fan, B. Xu, E. Gabrielsson, Q. Daniel, L. Li and L. Sun, *J Am Chem Soc*, 2015, **137**, 9153-9159.
3. Y. Yu, K. A. Click, S.-C. Chien, J. Sun, A. Curtze, L.-C. Lin and Y. Wu, *The Journal of Physical Chemistry C*, 2019, **123**, 8681-8687.
4. D. Wang, F. Niu, M. J. Mortelliti, M. V. Sheridan, B. D. Sherman, Y. Zhu, J. R. McBride, J. L. Dempsey, S. Shen, C. J. Dares, F. Li and T. J. Meyer, *Proceedings of the National Academy of Sciences*, 2019, DOI: 10.1073/pnas.1821687116.
5. Gaussian 09, Revision A.02, M. J. Frisch, G. W. Trucks, H. B. Schlegel, G. E. Scuseria, M. A. Robb, J. R. Cheeseman, G. Scalmani, V. Barone, B. Mennucci, G. A. Petersson, H. Nakatsuji, M. Caricato, X. Li, H. P. Hratchian, A. F. Izmaylov, J. Bloino, G. Zheng, J. L. Sonnenberg, M. Hada, M. Ehara, K. Toyota, R. Fukuda, J. Hasegawa, M. Ishida, T. Nakajima, Y. Honda, O. Kitao, H. Nakai, T. Vreven, J. A. Montgomery, Jr., J. E. Peralta, F. Ogliaro, M. Bearpark, J. J. Heyd, E. Brothers, K. N. Kudin, V. N. Staroverov, R. Kobayashi, J. Normand, K. Raghavachari, A. Rendell, J. C. Burant, S. S. Iyengar, J. Tomasi, M. Cossi, N. Rega, J. M. Millam, M. Klene, J. E. Knox, J. B. Cross, V. Bakken, C. Adamo, J. Jaramillo, R. Gomperts, R. E. Stratmann, O. Yazyev, A. J. Austin, R. Cammi, C. Pomelli, J. W. Ochterski, R. L. Martin, K. Morokuma, V. G. Zakrzewski, G. A. Voth, P. Salvador, J. J. Dannenberg, S. Dapprich, A. D. Daniels, O. Farkas, J. B. Foresman, J. V. Ortiz, J. Cioslowski, and D. J. Fox, Gaussian, Inc., Wallingford CT, 2009.
6. D. L. Ashford, M. K. Gish, A. K. Vannucci, M. K. Brennaman, J. L. Templeton, J. M. Papanikolas and T. J. Meyer, *Chemical Reviews*, 2015, **115**, 13006-13049.
7. A. D. Becke, *The Journal of Chemical Physics*, 1993, **98**, 1372-1377.